EurJIC
European Journal of Inorganic Chemistry

Research Article
doi.org/10.1002/ejic.202400076

Chemistry Europe
European Chemical Societies Publishing

www.eurjic.org

Assessing the Cooperating Ability of 6-Hydroxypicolinic Acid and Pyridyl-Amide Ligands in Palladium-Mediated C–H Activation

Cintya Pinilla[a] and Ana C. Albéniz*[a]

The behavior of 6-hydroxypicolinic acid (pic-6-OH) and pyridyl-amides as cooperating ligands in the C–H activation of arenes has been studied experimentally. When deprotonated, both compounds are chelating ligands and bear either a pyridone moiety or an *N*-acyl substituent that can assist the C–H cleavage in the same way as the successful bipyridone ligands and MPAAs do. In addition, they are easily available, commercially or via straightforward syntheses. Palladium complexes of formula $(NBu_4)[Pd(\kappa^2\text{-}O, N\text{-pic-6-O})(C_6F_5)py]$ (**2**) and $[Pd(\kappa^2\text{-}N, N\text{-py-}CH_2N(COCF_3)(C_6F_5)py]$ (**6**) have been synthesized and their decomposition in the presence of an arene gives the C_6F_5-arene coupling product, showing that the ligands enable the C–H activation of the arene (arene = pyridine, toluene, ethyl benzoate). The amount of C_6F_5-arene products observed leads to the following trend in cooperating ability: pic-6-OH > pyridyl-amide. DFT calculations on the pyridine activation are consistent with the experimental findings. The C–H activation does not occur for the isomeric complex $(NBu_4)[Pd(\kappa^2\text{-}O, N\text{-pic-4-O})(C_6F_5)py]$ (**4**) with the pyridone oxygen far from the metal, showing the involvement of this moiety in the C–H cleavage. The performance of these ligands in the direct arylation of arenes has been evaluated.

Introduction

Metal-ligand cooperation has been used in the last years as a strategy to facilitate the cleavage of crucial bonds in catalytic transformations, including the activation of the robust C–H bonds in the functionalization of hydrocarbons catalyzed by palladium complexes.[1] The latter processes have proved to be an attractive, more convenient and sustainable alternative to the conventional Pd-catalyzed cross coupling reactions, which generally use organic halides and main-group organometallics that need to be previously prepared from the parent hydrocarbons.[2–5] Metal-ligand cooperation in Pd-catalyzed C–H functionalizations occurs for ligands that bear a basic group in a suitable position of the molecule. This group assists in the activation of the C–H bond by being involved in a concerted metalation deprotonation (CMD) transition state and taking up the proton generated in the heterolytic C–H bond cleavage. This is represented in Figure 1 for two of the useful cooperating ligands in this field: The *N*-acyl monoprotected amino acids (MPAA, Figure 1, a),[6] and the chelating pyridone derivatives

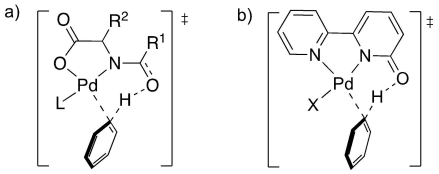

Figure 1. Transition states for the C–H activation with cooperating ligands: a) N-monoprotected amino acids (MPAA) and b) a bipyridone ligand (bipy-6-O).

such as bipy-6-OH in Figure 1, b.[7–10] The cooperation of the ligand decreases the energy of the C–H activation transition state, generally turnover limiting, and enables many functionalization reactions. These has been often supported by computational studies and we have devised an experimental approach that unequivocally shows if a ligand is capable of assisting the C–H cleavage of an arene. It is based on the synthesis of well-defined complexes of the target ligand that additionally bear an aryl group. When these complexes are thermally decomposed in the presence of an arene, the formation of the aryl-arene coupling product is a straightforward indication of the C–H activation of the arene. This is shown in Scheme 1 for bipy-6-OH,[7,8a] and MPAAs.[11]

We decided to apply this tool to other potential cooperating ligands of similar structure which have been little used in C–H functionalization reactions but could be interesting in this field. Taking into account the features that have made MPAAs and bipy-6-OH successful cooperating ligands in C–H activation, the cooperating ability of the related 6-hydroxypicolinic acid and pyridyl-amide type ligands is assessed in this work. Their structure comparison to the established cooperating ligands mentioned above can be seen in Figure 2.

[a] *Dr. C. Pinilla, Prof. Dr. A. C. Albéniz*
IU CINQUIMA/Química Inorgánica
Universidad de Valladolid
47071-Valladolid (Spain)
E-mail: albeniz@uva.es

Supporting information for this article is available on the WWW under https://doi.org/10.1002/ejic.202400076

Research Article
doi.org/10.1002/ejic.202400076

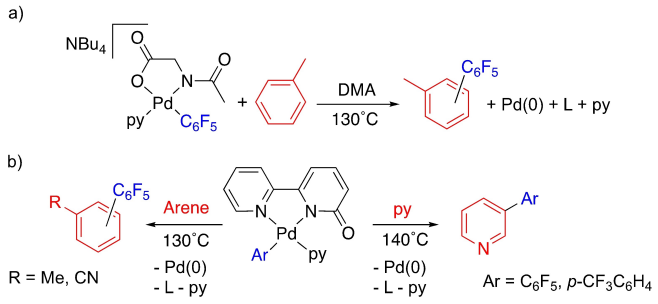

Scheme 1. Experimental evidence of the cooperation in the C–H activation of arenes of a coordinated MPAA (a) and bipy-6-OH (b).

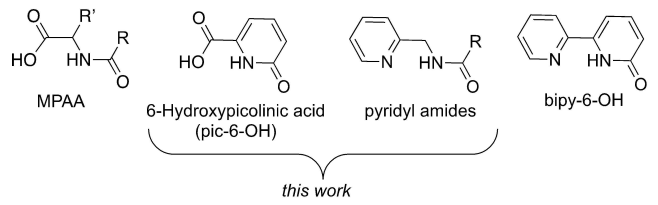

Figure 2. Structure comparison of the ligands used in this work to MPAAs and the bipyridone bipy-6-OH.

Upon double deprotonation 6-hydroxypicolinic acid can act as a dianionic ligand, as MPAA ligands can, but has a potentially cooperating pyridone moiety. In contrast with other chelating pyridone-type ligands, it is commercially available which is an attractive feature. This ligand, and its regioisomers, have been used coordinated to iridium for the oxidation of water,[12] and recently a similar derivative, has proved to be very effective in the Pd-catalyzed C–H hydroxylation of arenes.[13] Besides this example, the ligand has only been sporadically tested in C–H functionalization reactions.

The pyridyl-amide derivatives can be monoanionic ligands, as bipy-6-OH for example, but have a potentially cooperating acyl moiety, similar to the one in the MPAAs. The compounds have the advantage of a simple and modular synthetic route, *via* reaction of an amine and a carbonyl compound. There are a few precedents of the use of similar ligands, dubbed as acetyl-protected aminoethyl quinolines (APAQ), in C–H activation.[14,15] These ligands have an additional CHR linkage between the two N-donor atoms that, when coordinated, lead to a six-member ring metallacycle vs. five-member for all the derivatives mentioned here.

In order to achieve more efficient Pd-catalyzed C–H functionalization reactions it is important to identify the ligands that can be involved in metal-ligand cooperation in the C–H activation step, since this is commonly turnover limiting. We report here the independent evaluation of the ability of 6-hydroxypicolinic acid and a pyridyl-amide ligand to assist the C–H cleavage of arenes.

Results and Discussion

Pentafluorophenyl complexes with both ligands were prepared as specified below. The use of C_6F_5 is convenient to impart enough stability to the complexes, so they can be prepared and handled, as well as to monitor the reactions by ^{19}F NMR. The F_{ortho} chemical shifts change dramatically (about 20 ppm) when a Pd–C_6F_5 moiety is transformed into a C–C_6F_5 in the coupling products after the C–H activation, which unequivocally indicates the fate of the C_6F_5 group. The pentafluorophenyl group has shown analogous behavior to less fluorinated aryls in palladium-mediated C–C coupling processes,[16] and it is a good model to perform studies on isolated steps of catalytic reactions.[17]

6-Hydroxypicolinato Complexes and Cooperating Ability of the Ligand

6-Hydroxypicolinic acid (pic-6-OH) is diprotic and can be deprotonated to behave as a mono- and dianionic ligand. The reaction between two equivalents of pic-6-OH and the palladium dimer $(NBu_4)_2[Pd(\mu\text{-}Br)Br(C_6F_5)]_2$ in the presence of a base (mol ratio base:pic-6-OH = 1:1) produced a palladium complex with a monoanionic coordinated ligand as can be seen in Scheme 2. Complex **1** was obtained as a mixture of two different monomeric isomers (**1a** and **1b**), tentatively assigned to the cis-trans geometries, depending on the relative positions of the bromo atom and the pentafluorophenyl group. However, the geometry of each isomer could not be unequivocally assigned (mol ratio **1a**:**1b** = 1:0.4). The reaction of **1** (isomer mixture) with silver carbonate in the presence of pyridine led to complex **2** with the ligand in its dianionic form and coordinated as a chelate to the metal center (Scheme 2). A molecule of pyridine is coordinated to the vacant site produced after the abstraction of the bromine atom with the silver salt. The

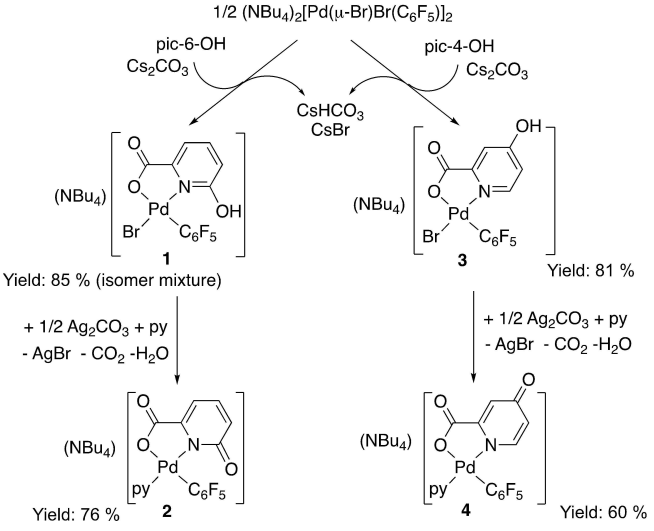

Scheme 2. Preparation of complexes **1**–**4**.

Research Article
doi.org/10.1002/ejic.202400076

structure of **2** was confirmed by the determination of its molecular structure by X-Ray diffraction (Figure 3).

The corresponding complexes of the regioisomeric 4-hydroxypicolinic acid (pic-4-OH) were also synthesized in the same manner (**3**, **4**, Scheme 2). These complexes bear the pyridone oxygen in a position far from the metal and a priori cannot be involved in a transition state similar to those in Figure 1.

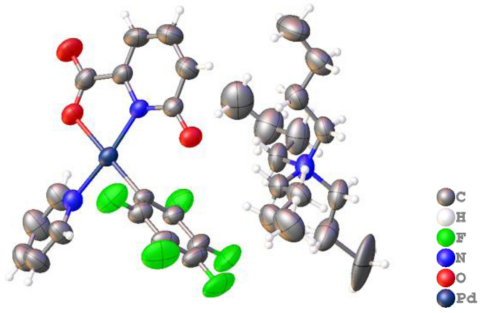

Figure 3. X-ray molecular structure of complex **2** (ORTEP plot, 40% probability ellipsoids).

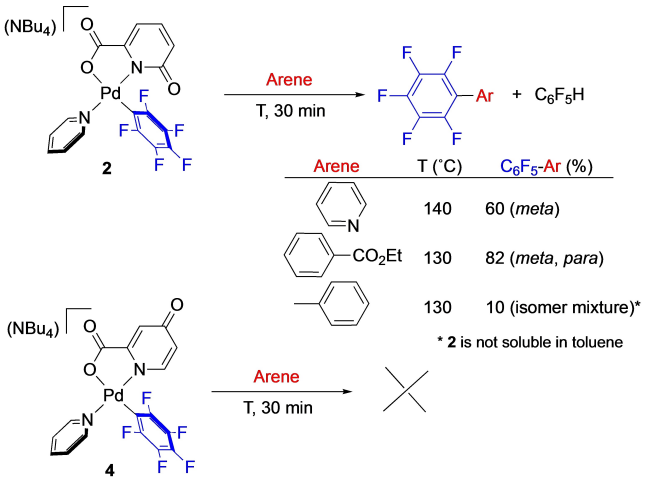

Scheme 3. Decomposition of complex **2** in different arenes.

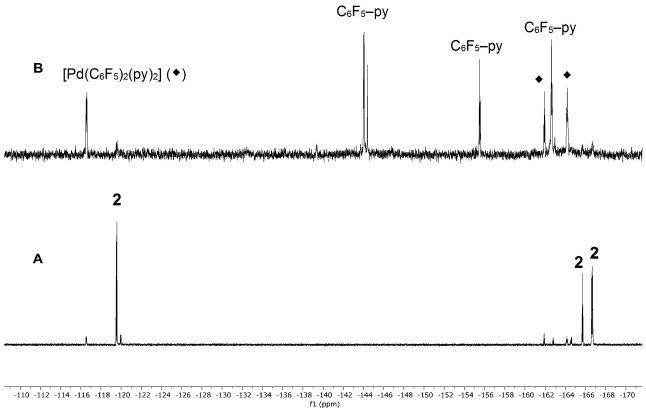

Figure 4. ^{19}F NMR spectra (470.168 MHz): A) Complex **2** in pyridine. B) Sample A after heating at 140 °C for 30 min (% mol: **2**, 7%; $[Pd(C_6F_5)_2(py)_2]$, 33%; *m*-C_6F_5-py, 60%).

The thermal decomposition of **2** in different arenes in the absence of any base, results in the formation of the arene-pentafluorophenyl coupling products showing that the ligand is capable of cooperating in the C–H bond cleavage (Scheme 3). This is clearly observed by the strong change in chemical shift for the F_{ortho} signals in the ^{19}F NMR spectra of the pentafluorophenyl group when bound to the metal or to a carbon (Figure 4).

In pyridine at 140 °C the coupling product *meta*-C_6F_5-py is formed in 60% after 30 min, as can be seen in Figure 4. The byproduct $[Pd(C_6F_5)_2(py)_2]$ formed by group reorganization between two different palladium complexes was also observed in a 30% yield. This reorganization is not uncommon for pentafluorophenyl derivatives,[11] and it occurs by transmetalation between palladium centers.[18]

In toluene, only 10% of the coupling product was observed after heating for 30 min. The extremely low solubility of complex **2** in toluene probably determines the slow rate of the C–H activation and the low amount of C_6F_5-tol. In contrast to pyridine as arene (*meta* coupling) the C–H activation of toluene is not selective and a mixture of regioisomers for the C_6F_5-tol coupling products was obtained (Figure S2, Supporting Information). This has been observed before for the C–H functionalization reactions with bipy-6-OH as cooperating ligand.[8a] Complex **2** is soluble in ethyl benzoate and 82% of the desired coupling products was obtained after heating a solution of **2** in this arene for 30 min. This demonstrates that the C–H activation of ethyl benzoate assisted by the ligand is possible in excellent yields (Figure S1, Supporting Information).

In contrast to complex **2** the regioisomeric complex **4** derived from 4-hydroxypicolinic acid does not lead to any coupling product with the arenes (Scheme 3 and Figures S3 and S4 in the Supporting Information). The pyridone oxygen is far from the metal in complex **4** and it cannot be involved in a CMD transition state such as those depicted in Figure 1, so the metal-ligand cooperation is not possible.

The C–H cleavage is usually the turnover limiting step for the direct arylation reactions, and this was found in the reported example for the direct arylation of pyridine with *p*-$CF_3C_6H_4I$ using bipy-6-OH as ligand (activation Gibbs energy 27.5 kcal mol^{-1}).[7] DFT calculations at the M06 level were carried out on the same system to compare the energy requirements for the C–H activation using pic-6-OH as cooperating ligand to those of the abovementioned system for bipy-6-OH (see Experimental Section and Supporting Information for details). The energy barrier for the dianionic pic-6-O was found to be 25.4 kcal mol^{-1}, slightly lower than that for bipy-6-O (Figure 5). This barrier is also in agreement with the conditions needed for the thermal decomposition of the preformed complex **2**, analogous to **I1** in Figure 5. It is clear that the ligand is able to cooperate in the C–H activation of the arene in the same way as the bipy-6-O ligand does.

Looking at the profiles in Figure 5, a similar ΔΔG is found between **I2** and **TS I2–I3**, the actual C–H cleavage, for pic-6-O and bipy-6-O (11 and 10.2 kcal mol^{-1} respectively). However a noticeable energy difference was found between the π-coordinated arene (**I2**) for pic-6-O and bipy-6-O, the former

Research Article
doi.org/10.1002/ejic.202400076

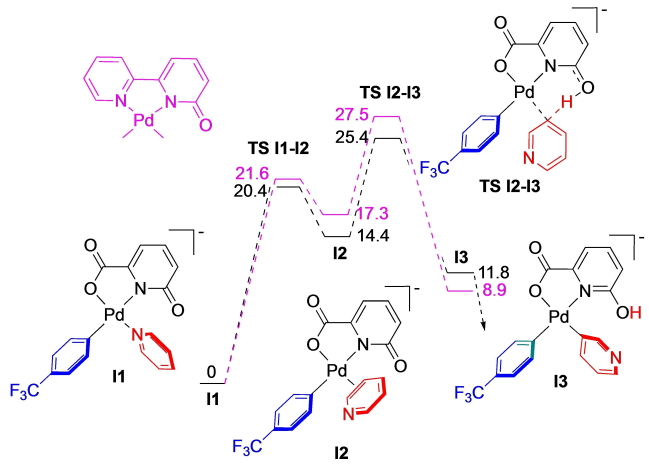

Figure 5. Gibbs energy profile for the pic-6-O assisted cleavage of the *meta* C–H bond of pyridine. The energy values for the analogous profile for bipy-6-O as ligand are also shown for comparison (data in magenta, taken from reference 7). Energies in kcal mol^{-1}.

being about 3 kcal mol^{-1} more stable. This can be explained by the lower trans influence of the carboxylate in pic-6-O *vs* the pyridine-fragment in bipy-6-O which leads to a stronger binding of the π-arene in the former case. The calculated Pd-π-arene distances are indeed a bit shorter for pic-6-O (Pd–C_{ortho}(π-pyridine): 2.402 Å, Pd–C_{meta}(π-pyridine): 2.338 Å) than for bipy-6-O (Pd–C_{ortho}(π-pyridine): 2.456 Å, Pd–C_{meta}(π-pyridine): 2.356 Å). Thus, the stability of **I2** is responsible for the lower energetic span in the overall C–H activation process which gives a small advantage to pic-6-O.

However, the performance of this ligand in the catalytic direct arylation of arenes does not surpass that of bipy-6-OH. Eq. 1 shows the general model reaction we used, and Table 1 collects different experiments using pyridine, toluene and ethylbenzoate as arenes under different conditions (see the Supporting Information for additional experiments).

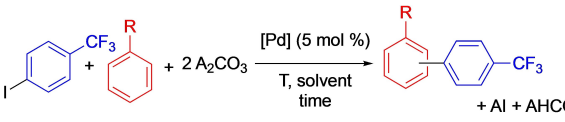

(1)

Either the mixture $Pd(OAc)_2$ and pic-6-OH or the preformed complex **2** are not active in the reactions under the same conditions as bipy-6-OH (entries 1–3, Table 1). In contrast with the latter system, we found that the use of a soluble carbonate base is crucial to achieve moderate yields of the final coupling product (entries 3–5, Table 1). The higher concentration of the base favors the complete deprotonation of the ligand, which then can be bound to the metal in the required chelating dianionic form prior to the C–H activation. The introduction of a polar and moderately coordinating co-solvent accelerate the reactions for toluene, as has been observed before,[8a] and has a beneficial effect in the direct arylation of pyridine (entries 6–8, Table 1). The reactions lead to significant amounts of the homocoupling product of the aryl halide used which seriously erodes the yield of the cross-coupling derivative.

Taking into account all the experiments done, it is clear that the ligand is able to assist in the C–H activation step as has been demonstrated by the thermal decomposition of complex **2** and supported by the DFT calculations. However, in the catalytic reaction does not work efficiently because the amount of byproducts formed by competitive reactions is really high and the coupling product is obtained in poor to moderate yields in all the cases, even in the best conditions when a co-solvent or soluble bases were used. This is in contrast to the related bipy-6-OH, which is highly efficient in these transformations. One of the major byproduct detected is the homocoupling derivative formed by the reorganization between two palladium aryl complexes prior to the C–H cleavage, i.e. intermediate **I1** (Figure 5) in the catalytic cycle or other palladium aryl species. This process involves the transmetalation of an aryl group from one palladium center to another in a dimer to form a bis-aryl complex and may be favoured by pic-6-O acting in different coordination modes, for example, as a

Table 1. Direct arylation reactions of pyridine, toluene and ethyl benzoate using *p*-$CF_3C_6H_4I$ and pic-6-OH as ligand according to Eq. 1.[a]

Entry	[Pd]	Base/ co-solvent	Pyridine[b]	Toluene[c]	Ethyl benzoate[c]
				Crude yield, % (conv., %), t (h)[d]	
1[e]	$Pd(OAc)_2$ + bipy-6-OH	Cs_2CO_3	96 (100), 2 h	20 (22), 6 h	84 (100), 6 h
2	$Pd(OAc)_2$ + pic-6-OH	Cs_2CO_3	0 (6), 6 h	3 (6), 6 h	10 (17), 6 h
3	**2**	Cs_2CO_3	5 (16), 6 h	2 (10), 6 h	3 (35), 6 h
4	**2**	$(NBu_4)CO_3Me$	35 (68), 2 h	20 (35), 2 h[f,g]	47 (99), 2 h[f]
5	**2**	$(NBu_4)_2CO_3$	48 (90), 2 h	23 (100), 6 h	47 (99), 2 h
6	**2**	$(NBu_4)CO_3Me$/DMA[h]	70 (100), 2 h		
7	**2**	$(NBu_4)_2CO_3$/DMA[h]	55 (100), 2 h		
8	**2**	$NBu_4)CO_3Me$/pinacolone[h]		28 (100), 2 h[f]	

[a] Reaction conditions: *p*-$CF_3C_6H_4I$ (0.34 mmol), arene as solvent (total volume 3.0 mL), [Pd] (5 mol%), base (0.68 mmol, except 0.34 mmol for pyridine,). [b] 140 °C; the meta regioisomer was obtained. [c] 130 °C; mixture of regioisomers. [b] Crude yields and conversion determined by ^{19}F NMR of the reaction mixture. The reduction of the ArI (ArH) and the homocoupling (Ar–Ar) are the observed byproducts. [e] Data taken from the literature (references 7, 8a). [f] Base (0.51 mmol). [g] 24% yield (98% conversion) after 24 h. [h] Co-solvent (1.5 mL) and arene (1.5 mL) as solvent mixture.

Research Article
doi.org/10.1002/ejic.202400076

transient κ^2-*O*, *O* monoanionic bridging ligand through the acetato group or in a monodentate form providing an available vacant site. Thus, the ligand cooperation in the C–H cleavage occurs when it is bound to the metal in a chelating κ^2-O, N dianionic mode and the importance of this is supported by the beneficial effect of a soluble base in the catalysis which favors the complete deprotonation of the ligand. Pic-6-OH can adopt a higher number of coordination modes than bipy-6-OH and this opens new reaction pathways that are detrimental for an efficient catalysis.

Pyridyl-Amide Complexes and Ligand Cooperation in the C–H Activation

Several pyridyl-amide ligands were synthesized by reaction of 2-aminomethyl pyridine or 8-aminoquinoline and the corresponding acyl chloride or carboxylic derivative (**L1**–**L6**, Figure 6). The model palladium pentafluorophenyl complexes **5** and **6** were also prepared in a similar way as that described above for the pic-6-OH derivatives (Figure 6).

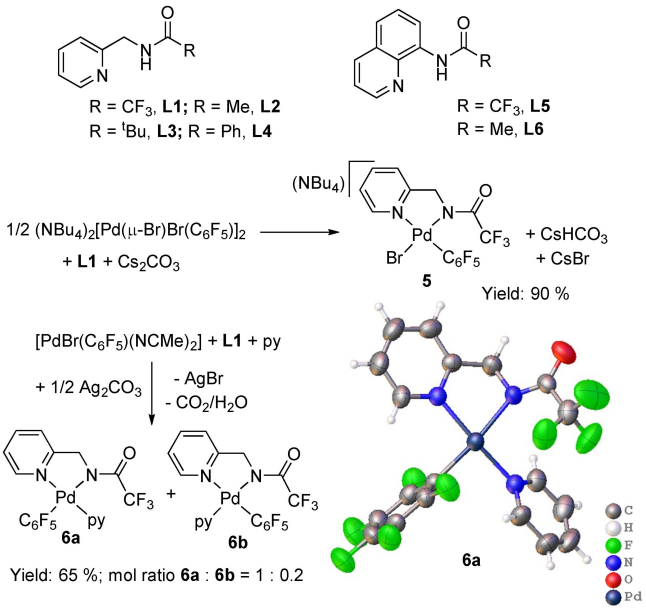

Figure 6. Amido-pyridie ligands used in this work and model complexes synthesized using **L1**. X-ray molecular structure of complex **6a** (ORTEP plot, 40% probability ellipsoids).

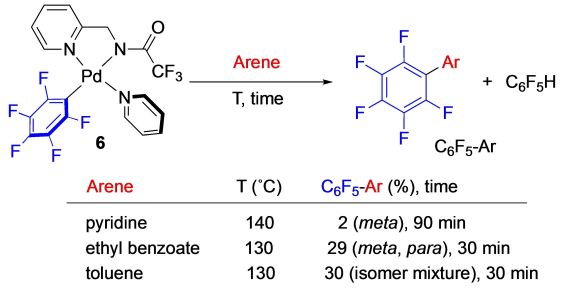

Arene	T (°C)	C_6F_5-Ar (%), time
pyridine	140	2 (*meta*), 90 min
ethyl benzoate	130	29 (*meta*, *para*), 30 min
toluene	130	30 (isomer mixture), 30 min

Scheme 4. Decomposition of complex **6** in different arenes.

Complex **6** was isolated as a mixture of cis and trans isomers (**6a** and **6b**). The stereochemistry of **6a** in solution was unequivocally determined by ^{1}H-^{19}F HOESY that shows the close proximity of: a) the pyridyl fragment of the chelating ligand to the F_{ortho} of the pentafluorophenyl group and b) the CF_3 group to the pyridine ligand (Figures S31–S32, Supporting Information). The molecular structure of complex **6a** was determined by X-ray diffraction and it is shown in Figure 6.

The thermal decomposition of complex **6** in different arenes was tested and the amount of the pentafluorophenyl-aryl coupling products was determined in each case (Scheme 4). This allows to evaluate the cooperating ability of the ligand.

When compared with the analogous pic-6-O complex (**2**, Scheme 3), it is clear that the pyridyl-amido ligand is more reluctant to enable the C–H activation of the arene. Only 2% of the coupling product with pyridine (*m*-C_6F_5-py) was observed in 90 min, three times longer than that needed to get 60% of *m*-C_6F_5-py for complex **2**. About 46% of the starting material remained, so the complex seems to be robust under the reaction conditions and the ligand does not decoordinate even in the presence of a large excess of pyridine (solvent). As mentioned above, both the reorganization complex [Pd-$(C_6F_5)_2(py)_2$] and C_6F_5H were observed as byproducts (Figure 7).

The pyridyl-amide ligand is capable of assisting the C–H cleavage of ethyl benzoate (Figure S6, Supporting Information) but, again, it is slower than pic-6-OH (29% of the coupling product after 30 min vs 82% for complex **2**). In contrast, the C–H activation of toluene is more effective for complex **6** (Figure S5, Supporting Information): 30% of the coupling product was formed after 30 min vs 10% for complex **2**, although this result is clearly influenced by the very low solubility of the pic-6-OH derivative in toluene whereas **6** is completely soluble.

DFT calculations on the pyridine system are consistent with the lower ability of the monoanionic ligand **L1** to assist the C–H cleavage (Figure 8). The barrier to reach the transition state for the C–H activation assisted by the ligand was found to be 35.5 kcal mol^{-1}, much more energy demanding than that for pic-6-O (25.4 kcal mol^{-1}, Figure 5) and the one reported in the

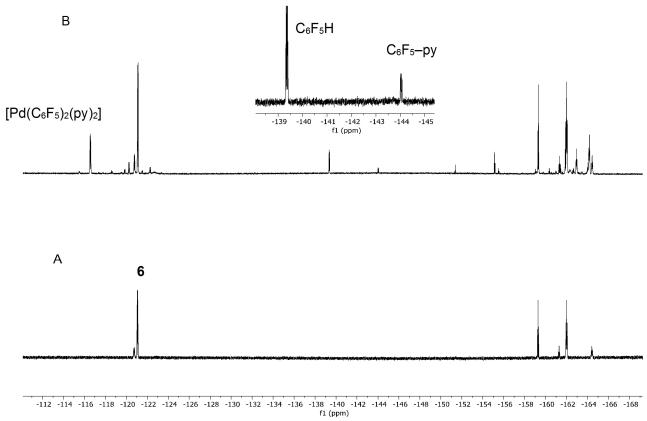

Figure 7. ^{19}F NMR spectra (470.168 MHz): A) Complex **6** in pyridine. B) Sample A after heating at 140 °C for 90 min (% mol: **6**, 46%; $[Pd(C_6F_5)_2(py)_2]$, 26%; C_6F_5-py, 2%; C_6F_5H, 10%). Only the F_{ortho} region is labeled for simplicity.

Research Article
doi.org/10.1002/ejic.202400076

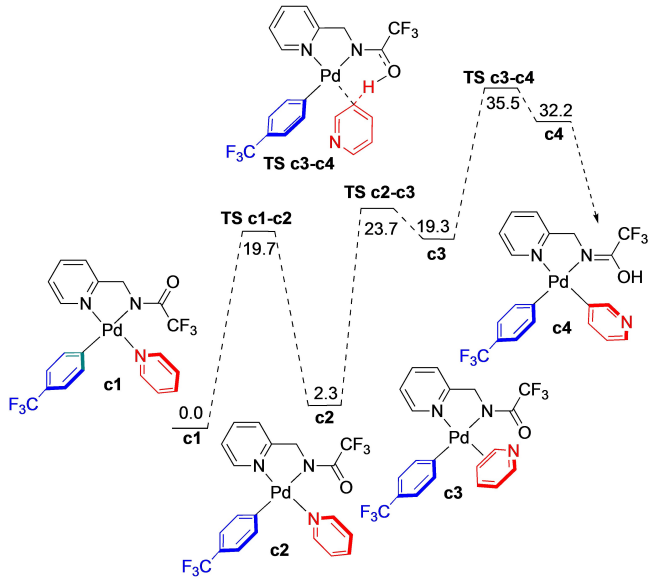

Figure 8. Gibbs energy profile for the assisted cleavage of the *meta* C–H bond of pyridine by the pyridyl-amide **L1**. Energies in kcal mol^{-1}.

literature for the ligand bipy-6-O (27.5 kcal mol^{-1}, Figure 5).[7] It is worth noting that **6a** bears the ketone group away from the metal, and the metal-ligand cooperation in a complex like this would not be possible. Thus, a rotation around the N–C(O) bond is needed and this was calculated. The barrier found (19.7 kcal mol^{-1}) is low enough for this rotation to occur much faster than the C–H activation. The rearrangement of the pyridine ring from a κ-*N* to a η^2-pyridine (activation energy 23.7 kcal mol^{-1}) is also accessible. In this case a higher ΔΔG is found between **c3** and **TS c3–c4** (16.3 kcal mol^{-1}) so the actual C–H cleavage is more energy demanding that for pic-6-O or bipy-6-O, which could be related to the lower basicity of the amido oxygen in **TS c3–c4** and the lower stability of the tautomeric form shown in **c4**.

The high activation energy of the process makes the C–H activation step slow for the pyridine ring and this type of ligands are inefficient in the direct arylation of pyridine. The catalytic reaction in Eq. 1 for pyridine led to very low yields both with complex **6** and with mixtures of $Pd(OAc)_2$/ligand (ligand = **L1**–**L6**) as catalysts (Table S4, Supporting Information). The direct arylation of ethyl benzoate and toluene with *p*-$CF_3C_6H_4I$ was also tested but, again, these ligands do not enable the reaction and only low yields of the cross coupling product were obtained (Tables S5 and S6, Supporting Information). No significant differences were observed for ligands **L1**–**L6**. The use of soluble bases for this monoanionic ligands has no beneficial effect on the reactions.

Conclusions

The ligand 6-hydroxypicolinic acid (pic-6-OH) and the pyridyl-amide type ligands coordinate to palladium in their chelating dianionic and monoanionic forms respectively and behave as cooperating ligands in the C–H activation reaction of arenes with different ability. This has been experimentally demonstrated by the thermal decomposition of isolated palladium complexes of the type $[Pd(C_6F_5)(ligand)(py)]^{n-}$ (**2**, **6**) in different arenes as solvent (pyridine, toluene and ethylbenzoate), that lead to the C_6F_5-arene coupling products. In contrast, the isomeric complex bearing a deprotonated 4-hydroxypicolinic acid (**4**) does not lead to the C_6F_5-arene products since the pyridone oxygen is far from the metal and it is not capable of metal-ligand cooperation. These experimental results, and the DFT calculations on the same system (arene = pyridine) along with data in the literature,[7] show the following trend in facilitating the C–H activation step: pic-6-O ≥ bipy-6-O > py-amide.

The performance of the ligand 6-hydroxypicolinic acid (pic-6-OH) in the catalytic direct arylation of arenes is improved when soluble carbonate bases are used, sometimes in conjunction with a co-solvent (DMA), which points to the importance of the chelating dianionic coordination mode of the ligand (favored by a higher base concentration) for an efficient C–H activation. However, even in these conditions, only moderated yields of the target products were observed in since the ligand seems to promote the formation of a high amount of byproducts, mainly the homocoupling derivative of the aryl halide.

The results for the direct arylation of arenes with pyridyl-amide ligands are poor. The direct arylation of pyridine is difficult since the C–H activation barrier is high for this type of ligands. However, even for other arenes that have shown a more efficient C–H activation step in the thermal decomposition of complex **6**, the catalytic reactions show again a high amount of byproducts indicating that the intermediates evolve through reorganization pathways leading to, for example, homocoupling products.

The cooperation of these ligands during the C–H cleavage is a fact as this step has been tested independently with isolated palladium complexes. The ligand cooperation in the C–H activation is a necessary but not sufficient requirement for an efficient C–H functionalization, as shown here for direct arylation reactions. In any case, the proved ability of these ligands in the C–H activation step makes them suitable candidates to be considered when developing new catalytic C–H functionalization reactions.

Experimental Section

General considerations: ^{1}H, $^{13}C\{^1H\}$ and ^{19}F NMR spectra were recorded on Agilent MR-400 or Agilent MR-500 spectrometers at the *Laboratorio de Técnicas Instrumentales* (LTI) of the UVa. Chemical shifts (in δ units, ppm) were referenced to $SiMe_4$ (^{1}H and ^{13}C) and $CFCl_3$ (^{19}F). The spectral data were recorded at 293 K unless otherwise noted. Homonuclear (^{1}H-COSY, ^{1}H-NOESY and ^{1}H-ROESY) and heteronuclear (^{1}H-^{13}C HSQC and HMBC, ^{19}F-^{13}C HSQC and HMBC and ^{1}H-^{19}F HOESY) experiments were used to help with the signal assignments. Elemental analyses were carried out in a Carlo Erba 1108 microanalyzer (at the Vigo University, Spain). HRMS analyses were carried out on a Bruker Maxis Impact mass spectrometer at the *Laboratorio de Técnicas Instrumentales* (LTI) of the UVa. Solvents

Research Article
doi.org/10.1002/ejic.202400076

Chemistry Europe
European Chemical Societies Publishing

were dried using a solvent purification system SPS PS-MD-5 (THF, hexane, CH_2Cl_2, Et_2O) or distilled from appropriate drying agents under nitrogen prior to use and stored over 3 Å or 4 Å molecular sieves (acetone, toluene, pyridine, DMA, ethyl benzoate, pinacolone). NEt_3 was dried, distilled and stored under nitrogen. 6-hydroxypicolinic acid, 4-hydroxypicolinic acid, alkali carbonates, potassium phosphate, $(NMe_4)Cl$, $(NBu_4)OAc$, $Pd(OAc)_2$ and the aryl iodide used are commercially available and were used as received unless otherwise indicated. $(NBu_4)_2[Pd_2(\mu\text{-}Br)_2Br_2(C_6F_5)_2]$,[19] and $[PdBr(C_6F_5)(NCMe)_2]$,[20] were synthesized according to the procedures in the literature.

Synthesis of pyridyl-amide ligands: In a two necked 100 mL flask 2-aminomethylpyridine, or 8-aminoquinoline (10 mmol), CH_2Cl_2 (20 mL) and NEt_3 (1.52 mL, 11 mmol) were added under nitrogen. The solution was cooled to 0 °C. The corresponding acid chloride, anhydride or acid (12 mmol) was added dropwise while stirring. The mixture was warmed to room temperature and stirred for 20 h. The solution was washed with water (3×5 mL), $NaHCO_3$ aq. (3×5 mL) and dried with $MgSO_4$. The solvent was evaporated in vacuo. The product was used without further purification in most cases. Additional information and NMR data for the ligands can be found in the Supporting Information.

(NBu_4)[PdBr(C_6F_5)(6-hydroxypicolinato)] (1): In a 100-mL flask 30 mL of acetone, 6-hydroxypicolinic acid (103 mg, 0.74 mmol), $(NBu_4)_2[Pd_2(\mu\text{-}Br)_2Br_2(C_6F_5)_2]$ (500 mg, 0.37 mmol) and Cs_2CO_3 (241 mg, 0.74 mmol) were introduced. The mixture was stirred at room temperature for 3 h. The suspension was filtered and the resulting solution was concentrated in vacuo affording a yellow oil. It was triturated with hexane and a yellow solid appeared. It was filtered and air-dried. Yield: 460 mg (85 %). The precipitate proved to be a mixture of two isomers in a ratio isomer **1 a**: isomer **1 b** = 1 : 0.4. Major isomer (**1 a**): ^{1}H NMR (500.13 MHz, δ, $(CD_3)_2CO$): 7.27 (br, 1H, H^4), 6.97 (br, 1H, H^3), 5.91 (d, J = 7 Hz, 1H, H^5), 3.45 (m, 8H, H^{NBu4}), 1.83 (m, 8H, H^{NBu4}), 1.43 (m, 8H, H^{NBu4}), 0.98 (t, J = 7.4 Hz, 12H, H^{NBu4}). $^{13}C\{^1H\}$ NMR (125.78 MHz, δ, $(CD_3)_2CO$): 172.5 (*C*OO) 168.6 (C^6), 152.6 (C^2), 138.2 (C^4), 116.6 (C^5), 114.3 (C^3), 58.5 (C^{NBu4}), 23.6 (C^{NBu4}), 19.5 (C^{NBu4}), 13.0 (C^{NBu4}). ^{19}F NMR (470.168 MHz, δ, $(CD_3)_2CO$): −118.2 (m, 2F, F_{ortho}), −168.7 to −170.8 (br, 3F, F_{para}, F_{meta}). Minor isomer (**1 b**): ^{1}H NMR (500.13 MHz, δ, $(CD_3)_2CO$): 10.5 (s, OH), 7.97 (t, J = 7.4 Hz, 1H, H^4), 7.51 (d, J = 7.0 Hz, 1H, H^3), 6.95 (d, J = 8.0 Hz, 1H, H^5), 3.45 (m, 8H, H^{NBu4}), 1.83 (m, 8H, H^{NBu4}), 1.43 (m, 8H, H^{NBu4}), 0.98 (t, J = 7.4 Hz, 12H, H^{NBu4}). $^{13}C\{^1H\}$ NMR (125.78 MHz, δ, $(CD_3)_2CO$): 173.3 (*C*OO), 165.5 (C^6), 150.0 (C^2), 142.0 (C^4), 118.3 (C^3), 114.6 (C^5), 58.5 (C^{NBu4}), 23.6 (C^{NBu4}), 19.5 (C^{NBu4}), 13.0 (C^{NBu4}). ^{19}F NMR (470.168 MHz, δ, $(CD_3)_2CO$): −119.7 (m, 2F, F_{ortho}), −164.7 (br, 1F, F_{para}), −167.3 (br, 2F, F_{meta}). HRMS (ESI-TOF): Calcd. for $C_{12}H_4BrF_5NO_3Pd$ $[M]^-$ 489.8335, found 489.8342.

(NBu_4)[Pd(C_6F_5)(6-oxidopicolinato)(py)] (2): In a 50-mL flask (NBu_4)[PdBr(C_6F_5)(6-hydroxypicolinate)] (**1**, 200 mg, 0.27 mmol) and 20 mL of acetone were introduced. Pyridine (90 μL, 1.1 mmol) and Ag_2CO_3 (37 mg, 0.14 mmol) were added. The mixture was stirred at room temperature for 20 h protected from light. It was filtered and the solution was concentrated in vacuo affording a yellow oil. It was triturated with hexane and a yellow solid precipitated. It was filtered and air-dried. Yield: 151 mg (76 %). Crystals suitable for X-ray analysis were obtained by slow evaporation of a solution of complex **2** in acetone at room temperature.

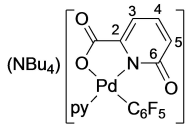

^{1}H NMR (500.13 MHz, δ, $(CD_3)_2CO$): 8.57 (m, 2H, $H^{ortho,py}$), 7.96 (tt, J = 7.7, 1.5 Hz, 1H, $H^{para,py}$), 7.47 (m, 2H, $H^{meta,py}$), 6.96 (dd, J = 6.5, 8.6 Hz, 1H, H^4), 6.44 (dd, J = 6.5, 1.5 Hz, 1H, H^3), 5.88 (dd, J = 8.6, 1.5 Hz, 1H, H^5), 3.42 (m, 8H, H^{NBu4}), 1.80 (m, 8H, H^{NBu4}), 1.42 (m, 8H, H^{NBu4}), 0.97 (t, J = 7.4 Hz, 12H, H^{NBu4}). $^{13}C\{^1H\}$ NMR (125.78 MHz, δ, $(CD_3)_2CO$): 173.4 (*C*OO)*, 167.8 (C^6)*, 153.8 (C^2)*, 152.2 ($C^{ortho,py}$), 147.8 (C^{Fo})*, 138.4 ($C^{para,py}$), 135.9 (C^{Fp})*, 135.5 (C^4), 134.9 (C^{Fm})*, 125.2 ($C^{meta,py}$), 120.5 (C^5), 120.3 ($C^{ipso,C6F5}$)*, 106.6 (C^3), 58.8 (C^{NBu4}), 23.3 (C^{NBu4}), 19.5 (C^{NBu4}), 13.1 (C^{NBu4}). ^{19}F NMR (470.168 MHz, δ, $(CD_3)_2CO$): −120.25 (m, 2F, F_{ortho}), −167.69 (t, J = 19.9 Hz, 1F, F_{para}), −168.28 (m, 2F, F_{meta}). HRMS (ESI-TOF): Calcd. for $C_{17}H_8F_5N_2O_3Pd$ $[M]^-$ 488.9502, found 488.9521. Anal. Calcd. For $C_{33}H_{44}F_5N_3O_3Pd$: C, 54.14 %; H, 6.06 %; N, 5.74 %. Found C, 53.65 %; H, 6.43 %; N, 5.25 %.

* The ^{13}C chemical shifts were determined by ^{1}H-^{13}C HMBC and ^{19}F-^{13}C HSQC.

(NBu_4)[PdBr(C_6F_5)(4-hydroxypicolinato)] (3): In a 100-mL flask 30 mL of acetone, 4-hydroxypicolinic acid (62 mg, 0.45 mmol), $(NBu_4)_2[Pd_2(\mu\text{-}Br)_2Br_2(C_6F_5)_2]$ (300 mg, 0.22 mmol) and Cs_2CO_3 (143 mg, 0.45 mmol) were introduced. The mixture was stirred at room temperature for 3 h. The suspension was filtered and the resulting solution was concentrated in vacuo affording an orange oil. It was triturated with hexane and an orange-yellow solid appeared which was filtered and air-dried. Yield: 131 mg (81 %). ^{1}H NMR (500.13 MHz, δ, $(CD_3)_2CO$): 7.12 (d, J = 3 Hz, 1H, H^3), 6.92 (d, J = 6.6 Hz, 1H, H^6), 6.39 (dd, J = 6.6, 3 Hz, 1H, H^5), 3.46 (m, 8H, H^{NBu4}), 1.82 (m, 8H, H^{NBu4}), 1.44 (m, 8H, H^{NBu4}), 0.98 (t, J = 7.4 Hz, 12H, H^{NBu4}). $^{13}C\{^1H\}$ NMR (125.78 MHz, δ, $(CD_3)_2CO$): 173.4 (C^4) 172.8 (*C*OO), 154.4 (C^2), 148.6 (C^6), 116.3 (C^3), 116 (C^5), 60.5 (C^{NBu4}), 23.6 (C^{NBu4}), 19.5 (C^{NBu4}), 13.0 (C^{NBu4}). ^{19}F NMR (470.168 MHz, δ, $(CD_3)_2CO$): −117.2 (m, 2F, F_{ortho}), −165.3 (t, J = 20.4 Hz, 1F, F_{para}), −166.9 (m, 2F, F_{meta}). HRMS (ESI-TOF): Calcd. for $C_{12}H_4BrF_5NO_3Pd$ $[M]^-$ 489.8335, found 489.8315.

NBu_4)[Pd(C_6F_5)(4-oxidopicolinato)(py)] (4): In a 50-mL flask (NBu_4)[PdBr(C_6F_5)(4-hydroxypicolinate)] (**3**, 82 mg, 0.11 mmol) was dissolved in acetone (20 mL). Pyridine (22 μL, 0.45 mmol) and Ag_2CO_3 (30.1 mg, 0.11 mmol) were added to the solution. The mixture was stirred at room temperature for 20 h protected from light. It was filtered and the solution was concentrated in vacuo affording a yellow oil. Cold Et_2O was added and a light yellow solid precipitated. It was filtered and air-dried. Yield: 64 mg (60 %).

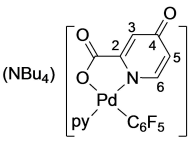

^{1}H NMR (500.13 MHz, δ, $(CD_3)_2CO$): 8.55 (d, J = 7.7 Hz, 2H, $H^{ortho,py}$), 8.02 (t, J = 7.7 Hz, 1H, $H^{para,py}$), 7.51 (t, J = 6.9 Hz, 2H, $H^{meta,py}$), 6.65 (d, J = 2.7 Hz, 1H, H^3), 6.51 (d, J = 7.2 Hz, 1H, H^6), 5.83 (dd, J = 7.2, 2.7 Hz, 1H, H^5), 3.45 (m, 8H, H^{NBu4}), 1.82 (m, 8H, H^{NBu4}), 1.44 (m, 8H, H^{NBu4}), 0.99 (t, J = 6.6 Hz, 12H, H^{NBu4}). $^{13}C\{^1H\}$ NMR (125.78 MHz, δ, $(CD_3)_2CO$): 177.9 (C^4) 173.0 (*C*OO), 153.7 (C^2), 152.4 ($C^{ortho,py}$), 148.1 (C^6), 138.9 ($C^{para,py}$), 125.6 ($C^{meta,py}$), 120.1 (C^3), 118.5 (C^5), 58.5 (C^{NBu4}), 23.5 (C^{NBu4}), 19.5 (C^{NBu4}), 12.9 (C^{NBu4}). ^{19}F NMR (470.168 MHz, δ, $(CD_3)_2CO$): −118.8 (m, 2F, F_{ortho}), −162.6 (t, J = 20.9 Hz, 1F, F_{para}), −164.4 (m, 2F, F_{meta}). The cross peaks between F_{ortho}-H^6 and F_{ortho}-$H^{ortho,py}$ in the ^{1}H-^{19}F HOESY NMR experiment allows to unequivocally assign the corresponding isomer. HRMS (ESI-TOF): Calcd. for $C_{17}H_8F_5N_2O_3Pd$ $[M]^-$ 488.9502, found 488.9501.

(NBu_4)[PdBr(C_6F_5)(2,2,2-trifluoro-*N*-(pyridin-2-ylmethyl)acetamide)] (5): In a 100-mL flask $(NBu_4)_2[Pd_2(\mu\text{-}Br)_2Br_2(C_6F_5)_2]$ (1.7 g, 1.25 mmol), 30 mL of acetone and 2,2,2-trifluoro-*N*-(pyridin-2-ylmethyl)acetamide (**L1**, 509 mg, 2.5 mmol)

Research Article
doi.org/10.1002/ejic.202400076

were introduced. Cs_2CO_3 (815 mg, 2.5 mmol) was added to the solution and the mixture was stirred at room temperature for 20 h. The solvent was evaporated in vacuo. EtOH (3 mL) and hexane (20 mL) were added to the orange oil which was stirred vigorously till a yellow solid appears. It was washed with hexane, filtered and air-dried. Yield: 1.8 g (90%). The complex is a single isomer and its structure was assigned based on the absence of cross-peaks in the ^{1}H-^{19}F HOESY experiment.

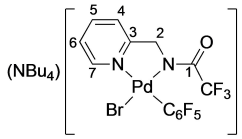

^{1}H NMR (500.13 MHz, δ, $(CD_3)_2CO$): 8.98 (d, J = 5.4 Hz, 1H, H^7), 7.95 (td, J = 1.7, 8.3 Hz, 1H, H^5), 7.58 (d, J = 8.3 Hz, 1H, H^4), 7.40 (m, 1H, H^6), 5.06 (s, 2H, H^2), 3.46 (m, 8H, H^{NBu4}), 1.83 (m, 8H, H^{NBu4}), 1.43 (m, 8H, H^{NBu4}), 0.98 (t, J = 7.2 Hz, 12H, H^{NBu4}). $^{13}C\{^1H\}$ NMR (125.78 MHz, δ, $(CD_3)_2CO$): 162.6 (C^1), 149.9 (C^7), 138.6 (C^6), 122.9 (C^5), 120.9 (C^4), 117.8 (q, $J_{C\text{-}F}$ = 288 Hz, CF_3), 58.5 (C^{NBu4}), 56.7 (C^2), 23.5 (C^{NBu4}), 19.4 (C^{NBu4}), 12.9 (C^{NBu4}). ^{19}F NMR (470.168 MHz, δ, $(CD_3)_2CO$): −70.43 (s, 3F, CF_3), −117.17 (m, 2F, F_{ortho}), −166.49 (t, J = 20.21 Hz, 1F, F_{para}), −168.57 (m, 2F, F_{meta}). HRMS (ESI-TOF): Calcd. for $C_{14}H_6BrF_8N_2OPd$ $[M]^-$ 554.8576, found 554.8573.

Pd(C_6F_5)(py)(2,2,2-trifluoro-*N*-(pyridin-2-ylmethyl)acetamido)] (6): In a 50-mL flask protected from light were introduced 15 mL of acetone, [PdBr(C_6F_5)($NCMe)_2$] (175 mg, 0.4 mmol), 2,2,2-trifluoro-N-(pyridin-2-ylmethyl)acetamide (**L1**, 82 mg, 0.4 mmol), pyridine (129.4 μL, 1.6 mmol) and Ag_2CO_3 (55.4 mg, 0.2 mmol). The mixture was stirred at room temperature for 20 h. A brown precipitate appeared and the suspension was filtered. The resulting yellow solution was evaporated in vacuo obtaining a yellow oil. Cold Et_2O was added and stirred till a yellow precipitate appeared. The precipitate was filtered and air-dried. Yield: 145 mg (65%). In acetone the solid proved to be a mixture of two isomers in a ratio at equilibrium (three days in solution) **a** (major): **b** (minor) = 1 : 0.2. The stereochemistry was determined by a ^{1}H-^{19}F HOESY NMR experiment: Isomer **a** shows cross peaks between F_{ortho}-$H^{ortho,py}$ and F_{ortho}-H^7, as well as a cross peak between F^{CF3}-$H^{ortho,py}$. Anal. Calcd. For $C_{19}H_{11}F_8N_3OPd$: C, 41.06%; H, 2.00%; N, 7.56%. Found C, 41.20%; H, 1.94%; N, 7.23%.

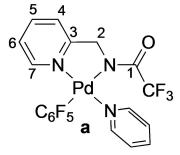

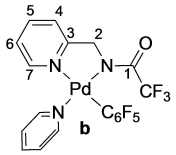

6a: ^{1}H NMR (500.13 MHz, δ, $(CD_3)_2CO$): 8.77 (d, J = 5.6 Hz, 2H, $H^{ortho,py}$), 8.03 (td, J = 8.0, 1.3 Hz, 1H, H^5), 7.98 (tt, J = 7.8, 1.8 Hz, 1H, $H^{para,py}$), 7.81 (d, J = 5.6 Hz, 1H, H^7), 7.74 (d, J = 8.0 Hz, 1H, H^4), 7.53 (m, 2H, $H^{meta,py}$), 7.28 (m, 1H, H^6), 5.17 (s, 2H, H^2). $^{13}C\{^1H\}$ NMR (125.78 MHz, δ, $(CD_3)_2CO$): 165.3 (C^1), 161.3 (C^3), 153.3 ($C^{ortho,py}$), 151.6 (C^7), 139.9 (C^6), 139.2 ($C^{para,py}$), 125.5 ($C^{meta,py}$), 123.6 (C^5), 122.0 (C^4), 54.7 (C^2). ^{19}F NMR (470.168 MHz, δ, $(CD_3)_2CO$): −71.99 (s, 3F, CF_3), −121.53 (m, 2F, F_{ortho}), −161.50 (t, J = 19.58 Hz, 1F, F_{para}), −163.68 (m, 2F, F_{meta}). The ^{13}C signals of the C_6F_5 and CF_3 groups, heavily coupled to ^{19}F, could not be located.

6b: ^{1}H NMR (500.13 MHz, δ, $(CD_3)_2CO$): 9.00 (d, J = 6.0 Hz, 2H, $H^{ortho,py}$), 8.11 (tt, J = 7.8, 1.6 Hz, 1H, $H^{para,py}$), 8.07 (m, 1H, H^5), 7.79 (d, J = 7.7 Hz, 1H, H^4), 7.68 (m, 2H, $H^{meta,py}$), 7.65 (t, J = 6.5 Hz, 2H, H^7), 7.38 (t, J = 6.6 Hz, 1H, H^6), 5.13 (s, 2H, H^2). $^{13}C\{^1H\}$ NMR (125.78 MHz, δ, $(CD_3)_2CO$): 153.1 ($C^{ortho,py}$), 146.78 (C^7), 139.6 (C^6), 126.1 ($C^{para,py}$), 126.7 ($C^{meta,py}$), 123.4 (C^5), 121.60 (C^4), 56.1 (C^2).* ^{19}F NMR (470.168 MHz, δ, $(CD_3)_2CO$): −70.50 (s, 3F, CF_3), −121.15 (m, 2F, F_{ortho}), −163.22 (t, J = 18.55 Hz, 1F, F_{para}), −166.10 (m, 2F, F_{meta}). * The remaining ^{13}C signals could not be located.

Thermal decomposition of 2, 4, and 6 in the presence of arenes: Complex **2** (7.3 mg, 0.01 mmol) was added into an NMR tube along with a sealed glass capillary filled with DMSO-d_6 as NMR lock signal. Then, 0.6 mL of the arene (pyridine, toluene or ethyl benzoate) as solvent were added. The solution was examined by ^{19}F NMR at room temperature. Then, the mixture was heated for the specified time. The experiment in toluene was done adding an internal standard (C_6F_6) due to the low solubility of **2**. The ^{19}F NMR signals of the decomposition products conform to those in the literature (see Supporting information).[7,8a] The decomposition experiments for complexes **4** and **6** were carried out in the same way.

General procedure for the catalytic direct arylation of arenes: $Pd(OAc)_2$ (3.8 mg, 0.017 mmol), the corresponding ligand (0.017 mmol) and base (0.68 mmol) were introduced in a Schlenk flask under a nitrogen atmosphere. Then, *p*-CF_3-C_6H_4I (0.34 mmol) and the specific arene (3.0 mL) or a mixture of arene (1.5 mL)/cosolvent (1.5 mL) were added to the flask. The reaction mixture was stirred at the specified temperature and checked by ^{19}F NMR of the crude mixture after 2 h, 6 h and 24 h. The spectroscopic data for the coupling products and byproducts were compared with the literature data.[7,8a] The results for the direct arylation reactions are collected in the Tables in the text and the Supporting Information.

Computational details. The DFT studies have been performed with the M06 functional,[21] as implemented in the Gaussian09 program package.[22] The 6-31 + G(d) basis set was used for C, O, N, F and H,[23] and LANL2TZ(f) for Pd,[24] (Basis set I). Solvent effects have been considered through the continuum model SMD for the experimental solvent, pyridine (ε = 12.3 at 25 °C), which was introduced in all the optimizations, frequency calculations and potential energy refinement. All structure optimizations were carried out in solvent phase with no symmetry restrictions. Gibbs energy corrections were calculated at 413.15 K (the experimental temperature) and 105 Pa pressure, including zero point energy corrections (ZPE), and the energies were converted to 1 M standard state in solution (adding/subtracting 1.89 kcal mol^{-1} for non-unimolecular processes). Vibrational frequency calculations were performed in order to confirm that the stationary points were minima (without imaginary frequencies) or transition states (with one imaginary frequency). Final potential energies were refined by performing additional single-point energy calculations (also in solution); Pd was still described with LANL2TZ(f) basis set, and the remaining atoms were treated with 6-311 + + G(d,p) basis set (Basis set II). All energies presented correspond to free energies in solution, obtained from potential energies (including solvation) with basis set II plus Gibbs energy corrections with basis set I and are given in kcal mol^{-1}.

Crrystallographic Details

Deposition Numbers 2329803 (for **2**) and 2329804 (for **6**) contain the supplementary crystallographic data for this paper. These data are provided free of charge by the joint Cambridge Crystallographic Data Centre and Fachinformationszentrum Karlsruhe Access Structures service.

Supporting Information

For additional experimental details, X-ray diffraction and computational data see the Supporting Information. The authors have cited additional references within the Supporting Information.[25,26]

Acknowledgements

We acknowledge the financial support of the Spanish MICIN (PID2022-142100NB-I00) and the Junta de Castilla y León-FEDER (VA087-18 fellowship to CP*)*, as well as the joint support of the EU/MICIN/JCyL (C17.I01.P01.S21, H_2MetAmo).

Conflict of Interests

The authors declare no conflict of interest.

Data Availability Statement

The data that support the findings of this study are available in the supplementary material of this article.

Keywords: C–H activation · metal-ligand-cooperation · palladium · pyridones · pyridyl-amides

[1] a) J. R. Khusnutdinova, D. Milstein, *Angew. Chem. Int. Ed.* **2015**, *54*, 12236–12273; b) T. Higashi, S. Kusumoto, K. Nozaki, *Chem. Rev.* **2019**, *119*, 10393–10402.
[2] a) T. Gensch, M. J. James, T. Dalton, F. Glorius, *Angew. Chem. Int. Ed.* **2018**, *57*, 2296–2306; b) T. Dalton, T. Faber, F. Glorius, *ACS Cent. Sci.* **2021**, *7*, 245–261.
[3] R. Vicente, A. R. Kapdi, L. Ackermann, *Angew. Chem. Int. Ed.* **2009**, *48*, 9792–9826.
[4] Y. Yang, J. Lan, J. You, *Chem. Rev.* **2017**, *117*, 8787–8863.
[5] a) J. He, M. Wasa, K. S. L. Chan, Q. Shao, J.-Q. Yu, *Chem. Rev.* **2017**, *117*, 8745–8786; b) M. J. Caplin, D. J. Foley, *Chem. Sci.* **2021**, *12*, 4646–4660.
[6] Q. Shao, K. Wu, Z. Zhuang, S. Qian, J. Q. Yu, *Acc. Chem. Res.* **2020**, *53*, 833–851.
[7] V. Salamanca, A. Toledo, A. C. Albéniz, *J. Am. Chem. Soc.* **2018**, *140*, 17851–17856.
[8] a) V. Salamanca, A. C. Albéniz, *Org. Chem. Front.* **2021**, *8*, 1941–1951; b) F. Villalba, A. C. Albéniz, *Adv. Synth. Catal.* **2021**, *363*, 4795–4804.
[9] Y. J. Wang, C. H. Yuan, D. Z. Chu, L. Jiao, *Chem. Sci.* **2020**, *11*, 11042–11054.
[10] Z. Wang, L. Hu, N. Chekshin, Z. Zhuang, S. Qian, J. X. Qiao, J.-Q. Yu, *Science* **2021**, *374*, 1281–1285.
[11] S. Fernández-Moyano, V. Salamanca, A. C. Albéniz, *Chem. Sci.* **2023**, *14*, 6688–6694.
[12] a) A. Bucci, A. Savini, L. Rocchigiani, C. Zuccaccia, S. Rizzato, A. Albinati, A. Llobet, A. Macchioni, *Organometallics* **2012**, *31*, 8071–8074; b) G. Menendez Rodriguez, A. Bucci, R. Hutchinson, G. Bellachioma, C. Zuccaccia, S. Giovagnoli, H. Idriss, A. Macchioni, *ACS Energy Lett.* **2017**, *2*, 105–110; c) B. Dijk, G. Menendez Rodriguez, L. Wu, J. P. Hofmann, A. Macchioni, D. G. H. Hetterscheid, *ACS Catal.* **2020**, *10*, 4398–4410; d) G. Menendez Rodriguez, F. Zaccaria, S. V. Dijk, C. Zuccaccia, A. Macchioni, *Organometallics* **2021**, *40*, 3445–3453.
[13] Z. Li, H. S. Park, J. X. Qiao, K.-S. Yeung, J.-Q. Yu, *J. Am. Chem. Soc.* **2022**, *144*, 18109–18116.
[14] G. Chen, W. Gong, Z. Zhuang, M. S. Andrä, Y.-Q. Chen, X. Hong, Y.-F. Yang, T. Liu, K. N. Houk, J.-Q. Yu, *Science* **2016**, *353*, 1023–1027.
[15] a) Y.-F. Yang, X. Hong, J.-Q. Yu, K. N. Houk, *Acc. Chem. Res.* **2017**, *50*, 2853–2860; b) Y.-F. Yang, G. Chen, X. Hong, J.-Q. Yu, K. N. Houk, *J. Am. Chem. Soc.* **2017**, *139*, 8514–8521; c) D. E. Hill, Q.-L. Pei, E.-X. Zhang, J. R. Gage, J.-Q. Yu, D. G. Blackmond, *ACS Catal.* **2018**, *8*, 1528–1531; d) E. A. Romero, G. Chen, M. Gembicky, R. Jazzar, J.-Q. Yu, G. Bertrand, *J. Am. Chem. Soc.* **2019**, *141*, 16726–16733.
[16] a) A. C. Albéniz, P. Espinet, B. Martín-Ruiz, D. Milstein, *J. Am. Chem. Soc.* **2001**, *123*, 11504–11505; b) S. Martínez-Arranz, N. Carrera, A. C. Albéniz, P. Espinet, A. Vidal-Moya, *Adv. Synth. Catal.* **2012**, *354*, 3551–3560.
[17] a) P. Espinet, A. C. Albéniz, J. A. Casares, J. M. Martínez-llarduya, *Coord. Chem. Rev.* **2008**, *252*, 2180–2208; b) F. Villalba, A. C. Albéniz, *Dalton Trans.* **2022**, *51*, 14847–14851.
[18] a) A. L. Casado, J. A. Casares, P. Espinet, *Organometallics* **1997**, *16*, 5730–5736; b) A. C. Albéniz, P. Espinet, O. López-Cimas, B. Martín-Ruiz, *Chem. Eur. J.* **2005**, *11*, 242–252.
[19] P. Espinet, A. C. Albéniz, R. Usón, J. Forniés, J. A. Nalda, M. J. Lozano, *Inorg. Chim. Acta* **1989**, *156*, 251–256.
[20] A. C. Albéniz, P. Espinet, C. Foces-Foces, F. H. Cano, *Organometallics* **1990**, *9*, 1079–1085.
[21] a) Y. Zhao, D. G. Truhlar, *J. Chem. Phys.* **2006**, *125*, 194101–194118; b) Y. Zhao, D. G. Truhlar, *Theor. Chem. Acc.* **2006**, *120*, 215–241.
[22] Gaussian 09, Revision D.01, M. J. Frisch, G. W. Trucks, H. B. Schlegel, G. E. Scuseria, M. A. Robb, J. R. Cheeseman, G. Scalmani, V. Barone, G. A. Petersson, H. Nakatsuji, X. Li, M. Caricato, A. Marenich, J. Bloino, B. G. Janesko, R. Gomperts, B. Mennucci, H. P. Hratchian, J. V. Ortiz, A. F. Izmaylov, J. L. Sonnenberg, D. Williams-Young, F. Ding, F. Lipparini, F. Egidi, J. Goings, B. Peng, A. Petrone, T. Henderson, D. Ranasinghe, V. G. Zakrzewski, J. Gao, N. Rega, G. Zheng, W. Liang, M. Hada, M. Ehara, K. Toyota, R. Fukuda, J. Hasegawa, M. Ishida, T. Nakajima, Y. Honda, O. Kitao, H. Nakai, T. Vreven, K. Throssell, J. A. Montgomery, Jr., J. E. Peralta, F. Ogliaro, M. Bearpark, J. J. Heyd, E. Brothers, K. N. Kudin, V. N. Staroverov, T. Keith, R. Kobayashi, J. Normand, K. Raghavachari, A. Rendell, J. C. Burant, S. S. Iyengar, J. Tomasi, M. Cossi, J. M. Millam, M. Klene, C. Adamo, R. Cammi, J. W. Ochterski, R. L. Martin, K. Morokuma, O. Farkas, J. B. Foresman, D. J. Fox, Gaussian, Inc., Wallingford CT, 2009.
[23] a) M. M. Francl, W. J. Pietro, W. J. Hehre, J. S. Binkley, M. S. Gordon, D. J. DeFrees, J. A. Pople, *J. Chem. Phys.* **1982**, *77*, 3654–3665; b) T. Clark, J. Chandrasekhar, G. W. Spitznagel, P. V. R. Schleyer, *J. Comput. Chem.* **1983**, *4*, 294–301.
[24] a) A. W. Ehlers, M. Böhme, S. Dapprich, A. Gobbi, A. Höllwarth, V. Jonas, K. F. Köhler, R. Stegmann, A. Veldkamp, G. Frenking, *Chem. Phys. Lett.* **1993**, *208*, 111–114; b) L. E. Roy, P. J. Hay, R. L. Martin, *J. Chem. Theory Comput.* **2008**, *4*, 1029–1031.
[25] a) C. C. Cody, H. R. Kelly, B. Q. Mercado, V. S. Batista, R. H. Crabtree, G. W. Brudvig, *Inorg. Chem.* **2021**, *60*, 14759–14764; b) A. Mondal, Y. Li, M. A. Khan, J. H. Ross, R. P. Houser, *Inorg. Chem.* **2004**, *43*, 7075–7082; c) U. P. Chaudhuri, L. R. Whiteaker, L. Yang, R. P. Houser, *Dalton Trans.* **2006**, 1902–1908; d) S. Kerdphon, X. Quan, V. S. Parihar, P. G. Andersson, *J. Org. Chem.* **2015**, *80*, 11529–11537; e) T. Yang, X. Cao, X.-X. Zhang, Y. Ou, C.-T. Au, S.-F. Yin, R. Qiu, *J. Org. Chem.* **2020**, *85*, 12430–12443; f) M. Pérez-Gómez, H. Azizollahi, I. Franzoni, E. M. Larin, M. Lautens, J. A. García-López, *Organometallics* **2019**, *38*, 973–980; g) C.-T. Yang, Y. Fu, Y.-B. Huang, J. Yi, Q.-X. Guo, L. Liu, *Angew. Chem. Int. Ed.* **2009**, *48*, 7398–7401.
[26] a) CrysAlisPro Software system, version 1.171.33.51, **2009**, Oxford Diffraction Ltd, Oxford, UK; b) G. M. Sheldrick, *Acta Crystallogr.* **2015**, *C71*, 3–8; c) O. V. Dolomanov, L. J. Bourhis, R. J. Gildea, J. A. K. Howard, H. Puschmann, *J. Appl. Crystallogr.* **2009**, *42*, 339–341.

Manuscript received: February 5, 2024
Revised manuscript received: April 14, 2024
Accepted manuscript online: April 17, 2024
Version of record online: May 23, 2024